Investigation of Void-free Chip-to-Chip Bonding Methods for CMOS-MEMS Compatibility

Yi Xuan Yeo, Eva Leong Ching Wai, Daniel Ssu-Han Chen, Ser Choong Chong
Institute of Microelectronics (IME), Agency for Science, Technology and Research (A*STAR), Singapore
11 Science Park Road 2, Singapore 117685
yeo_yi_xuan@ime.a-star.edu.sg

Abstract

A thin bonding interface that is void-free and composed of materials with low attenuation is needed to achieve GHz bulk acoustic wave signal transmission for analog computing accelerators. The presence of voids in the bonding interface would have significant attenuation of acoustic transmission, which often results in complete reflection of the acoustic signal. Thus, we aimed to develop a bonding process via heterogeneous integration involving MEMS and CMOS components, with a total absence of air bubbles between the bonded surfaces in the ambient air process. This paper presents the use of various methods including preform and thermocompression bonding to facilitate void-free bonding, enabling low attenuation for acoustic transmission through the sample and die-attach layers. From the results, it was found that TCB between Au and AuSn surface resulted in the least loss of signal.

Introduction

Chip-level bonding is ubiquitous in various heterogeneous integrations (HI), whereupon it is used to establish electrical connections between the chip and package, signal transmission, power delivery and heat dissipation. With a demand for micro-electro-mechanical systems (MEMS) and complementary metal-oxide-semiconductor (CMOS) components to achieve bulk acoustic wave (BAW) signal transmission for analog computing accelerators, there is a need for better bonding methods to ensure minimal loss of acoustic signals [1-3].

Noteworthy prior research includes the structural analysis conducted by H. K. Kim and N.H. Kim on Au-Au wafer bonding interfaces, confirming the viability of gold-to-gold (Au-Au) bonding [4]. Additionally, M. Yamamoto *et al.* explored the application of Ar+H_2 plasma treatment at atmospheric pressure (AP), demonstrating its significant enhancement of bonding strength in Au-Au bonding [5]. Likewise, S. Matsuoka *et al.* investigated the effects of N_2 and Ar+O_2 plasma cleaning processes at AP on Au-Au bonding [6]. Both studies showed that plasma cleaning of the surfaces enhances surface activated bonding (SAB), which was confirmed by the increase in shear strength. In line with these findings, our research also incorporated plasma cleaning into our bonding process and assessed the strength of the various bonding methods through shear testing.

This study was undertaken to address the demand for lossless acoustic transmission and to address the existing gap in research pertaining to void-free metallic surface bonding, thereby contributing to the advancement of bonding techniques essential for achieving optimal acoustic signal transmission.

Methodology

A total of five methods were investigated to achieve void-free bonding for BAW signal transmission. The first is using an indium (In) preform film reflowed to bond two silicon chips together. The second method is a similar process using gold-tin (AuSn) preform instead. The third is using a pressure-less silver (Ag) sintering paste. The fourth is direct thermocompression bonding (TCB) between the Au-Au metal surfaces of the 2 chips. The fifth method is the same as the fourth, but with surfaces of Au-to-AuSn.

Post-bonding, all samples underwent X-ray examination, and a subset underwent further analysis via C-mode Scanning Acoustic Microscopy (CSAM) to inspect the bonded layers. Among the samples subjected to CSAM, a portion was selected for die shear testing to assess the bonded layer and the strength of the bonding. As highlighted in [3], CSAM and X-ray analysis are insufficient to inspect micro-voids which can greatly impact the GHz acoustic signal transmission. As such, samples that were inspected to be void-free with X-ray and CSAM were further investigated by repeating the bonding methodologies with GHz MEMS devices for acoustic transmission evaluation. These MEMS devices are BAW transducers that can be used to evaluate the bonding quality by pulse-echo signal analysis [3].

For the first method, two 10×10 mm silicon dies with Au (150 nm)/Ti (50 nm) coating were stacked onto one another with the Indium preform in between using a pick and place tool (Fig. 1). A force of 4.5 kg was applied onto the stack to ensure adhesion of the perform and the dies. Subsequently, the stack was then placed in a reflow oven and reflowed at 170°C.

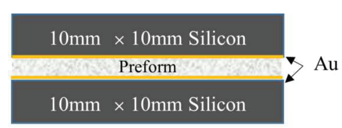

Fig. 1. Representation of die stack using methods 1 and 2 (Indium and AuSn preforms).

For the second method, the indium preform was replaced with AuSn preform, whilst the same Au-coated Si dies were used (Fig. 1). The pick and place procedure from the first method was used but at a higher temperature of 330ºC to ensure melting of the preform. However, there were still large voids in the die attached layer. The voids may have formed due to a lack of force applied onto the stack, hence direct heating during the stacking was employed. To achieve direct reflow of the preform, a flip-chip bonder was used. Two samples were prepared for each chosen higher temperature value (320°C, 350°C, 380°C), at a force of 0.4 kg and 1 kg, respectively.

For the third method, a pressure-less Ag sintering paste was used to bond an 8×8 mm MEMS die onto a silicon die. The paste was dispensed onto the bottom die surface and then the other was picked and placed on top of the bottom die. When placing, a force was applied to ensure the paste spread across the area of contact. The stack was cured in the batch oven at 220°C.

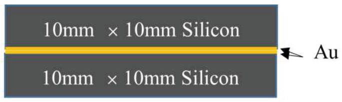

Fig. 2. Representation of die stack using method 4, Au-Au TCB.

For the fourth method, direct thermocompression bonding (TCB) was used with the flip-chip bonder for Au-Au bonding (Fig. 2). The 10×10 mm silicon dies were coated on one side with Ti (50 nm)/ Au (150 nm) layers via e-beam evaporation. To ensure void-free bonding, the surfaces had to be very clean, plasma cleaning was done, and the dies were then cleaned with IPA before bonding. The force applied by the bonder was 40 kg at 400°C. The variations tested were types of plasma (none, N_2, and $Ar+O_2$) and bonding time (50s, 120s, 180s) which gives a total of 9 samples.

Fig. 3. Representation of die stack using method 5, Au-AuSn TCB.

For the fifth method, TCB with Au-AuSn dies were bonded using the same flip-chip bonder (Fig. 3). The 8×8 mm MEMS dies were coated with Ti/Au on their underside via e-beam evaporation. For the AuSn dies, the 10×10 mm Si dies were coated with AuSn via e-beam evaporation with Ti/Au on one side, and Ti (20nm)/Sn (120nm)/Au (20nm) on the other. The Ti/Au surface of the MEMS die would be in contact with the Ti/Sn/Au surface of the Si die. Similarly, the dies were plasma cleaned with $Ar+O_2$ plasma, then cleaned with IPA. For the bonding, the temperature applied ranged from 240°C to 300°C, while a consistent force of 40 kg was applied across all samples. The duration of temperature applied, and force applied were varied to find the optimal parameters where the samples had high shear strength and minimal acoustic transmission loss.

Results

The fifth method using Au-AuSn had the best results, achieving void-free TCB between the die surfaces, whilst allowing GHz BAW signal transmission through the sample.

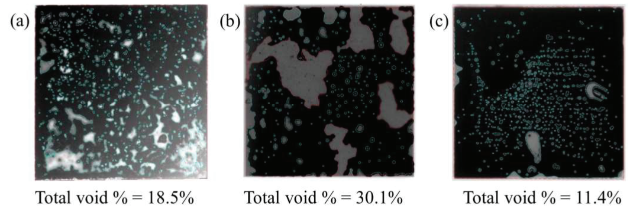

Fig. 4. X-ray images of samples bonded with preform and reflowed in a dispatch oven. (a) Indium (In) preform, void formed was the least amongst the indium samples at 18.5%. (b) Indium preform, void formed was the largest at 30.1%. (c) AuSn preform, void formed was 11.4%.

For the preform methods 1 & 2, significant void formations were observed in the bonded area (Fig. 4). Samples built using indium preform had void formations between 18.5% to 30.1% (Fig. 4(a) and 4(b)). Using the same pick and place tool, followed by reflow in the batch oven, samples built with AuSn preform had a lower void percentage at 11.4% (Fig. 4(c)). Despite efforts to use a flip-chip bonder with AuSn samples to mitigate void formation, X-ray examination revealed no obvious reduction of the solder voids. However, there were noticeable areas of the preform that did not reflow, even with constant force applied during the reflow process. Subsequent shear testing further confirmed the presence of intact preforms when the dies were separated. The summarized X-ray, CSAM, and shear test results are provided in Table 1. Given the inability of this preform method to achieve void-free bonding, it was ultimately deemed unsuitable for further consideration.

Table 1. AuSn preform samples built using a flip-chip bonder with 1 kg force and their corresponding X-ray image, CSAM, and shear test. Temperature applied for each sample: No. 1 at 320°C, No. 2 at 350°C, No. 3 at 380°C.

No	X-ray	CSAM	Shear Test	Shear strength
1	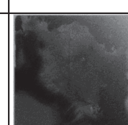	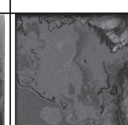		24.9 kg
2	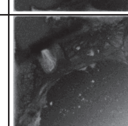	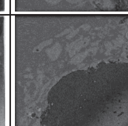	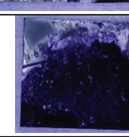	34.9 kg
3	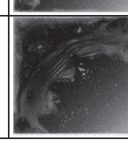	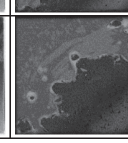	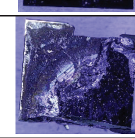	44.7 kg

In the case of the pressure-less Ag sintering paste method, minimal voids were observed, as illustrated in Fig. 5, with a mere 1.8% occurrence. This is in stark contrast to the void formations observed in samples constructed using preforms, as depicted in Fig. 4. Despite the promising reduction in voids, the presence of the miniscule air bubbles scattered across the sinter layer affected the signal transmission, resulting in the absence of any favorable electro-acoustic test. Therefore, due to the lack of acoustic transmission through the Ag sintering layer, this method was deemed unsuitable and subsequently discarded from further consideration.

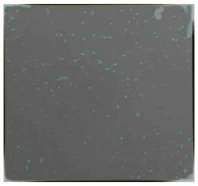

Fig. 5. X-ray image of the 8×8 mm MEMS chip die-attached using Ag sintering paste on Au-coated silicon die. Void formation was ~1.8%.

(a)

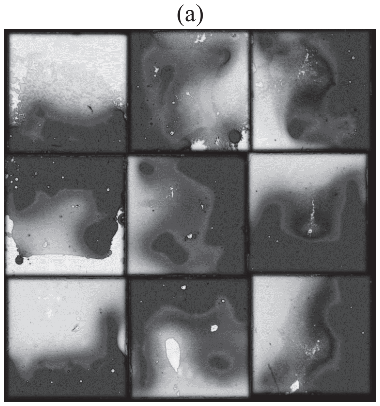

(b)

Fig. 6. (a) X-ray image of the Au-Au sample, no observable voids found via X-ray imaging for all the samples. (b) CSAM results for 9 samples, where the lighter areas are voids.

In the case of the TCB methods utilizing Au-Au samples, X-ray examination indicated a void-free bond (Fig. 6(a)). However, when observed using CSAM, unbonded areas were seen (Fig. 6(b)). This observation was further confirmed during the die shear test, which revealed areas where the Au was not bonded. This aligns with the results in Table 1, where the Au-coated surfaces of the dies remained intact, showing no signs of bonding. The unbonded areas corresponded to the lighter areas shown by the CSAM images.

For Au-AuSn bonding, the bonded layer exhibited greater uniformity, yielding positive acoustic results. As indicated in Table 2, the samples shown have large bonded areas with minimal voids. Sample No. 4 was bonded at 40kgf with chuck set at 200^{o}C and bond tool at 300^{o}C for duration of 300s. From the CSAM results in Table 2, it is evident that No. 4 had unbonded areas circled in red, which exhibited no acoustic transmission when tested. However, the remaining areas demonstrated positive acoustic results.

For sample No. 5, the same heating and force parameters were applied, but the compression duration was extended to 630s, in an attempt to achieve a more uniform bonding. The CSAM result for No. 5 revealed a more uniformly bonded layer, which was supported by the acoustic results, apart from the top left area where it was unbonded. It also had the highest shear strength amongst the Au-AuSn samples.

Sample No. 6 used the same parameters as sample No. 5 but with a variation in the force, and duration. While the temperature was maintained for 600s, the force was held for 300s. From the CSAM image in Table 2, the top right of sample No. 6 was unbonded. The shear strength results showed that the bonding of the dies was sufficient, as they were consistently above 10 kg.

A comprehensive assessment was conducted at a total of 32 measurement sites employing the electro-acoustic methodology described in [3]. The resulting data was categorized into three distinct classifications: "excellent," "good," and "poor”. Excellent indicates the reflected acoustic signal from the bonded interface was minimal and most of the signal has been transmitted to the bottom substrate. Good denotes there are some acoustic signals being reflected at the bonding interface, but the majority of the acoustic signal has been propagated to the substrate below. Poor signifies there are some signs showing acoustic signals being propagated, however, the signal has been attenuated at the bonding interface or completely reflected like an unbonded case which yields useless. Details of the acoustic transmission analysis based on pulse-RF technique are described in [2-3].

Table 2. CSAM results of Au-AuSn bonding, measured sites with the quality of acoustic transmission and associated shear strengths

No	**CSAM**	**Number of sites showing GHz acoustic transmission**			**Shear strength**
		Excellent	**Good**	**Poor**	
4	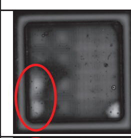	3	8	21	12.6 kg
5	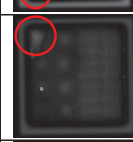	2	14	16	15.2 kg
6		0	10	22	13.2 kg

A summary of the electro-acoustic measurement results for samples No. 4 to 6 is illustrated in Fig. 7. On the sites where the acoustic transmission signal shows results in the “excellent” category in sample No. 4, a destructive wave in the second echo signal can be seen due to the resultant wavefront from the top chip surface and bottom chip surface reflections (Fig. 7(a)). On the sites where the acoustic transmission signal shows results in the “good” category in sample No. 5, the first echo signal is less than the second echo signal (Fig. 7(b)). This signifies that there is a strong indication that the acoustic signal has been propagated through the bonding interface which caused the second echo to be larger. In comparison, sample No. 6 with sites showing in the "good" category had similar echo profiles. However, the echo signals are weaker, and a smaller number of echoes can be identified (Fig. 7(c)).

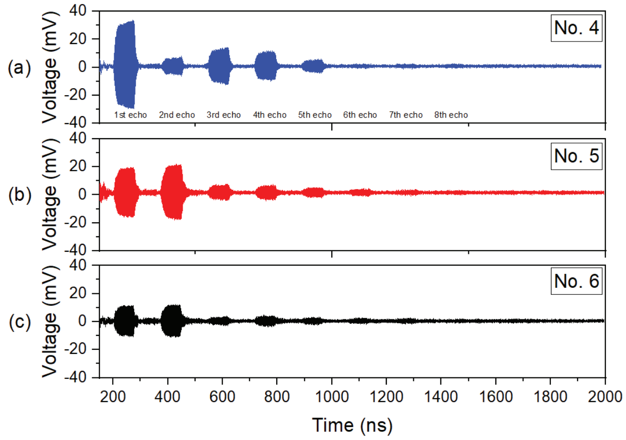

Fig. 7. Electro-acoustic measurement of (a) sample No. 4, (b) sample No. 5, (c) sample No. 6.

Conclusions

Based on the results obtained, direct TCB between Au-AuSn had achieved the least voids in the bonding layer. This allowed the signal to transmit with minimal losses. There is a high requirement for the flatness and cleanliness of the bonded surfaces so that the bonding would be free of debris and would not have a void due to the unevenness of the deposited surface.

Acknowledgments

This research is supported by A*STAR RIE2020 Advanced Manufacturing and Engineering Programmatic under the "Ultrasonic Wavefront Computing" grant (A19E8b0102).

References

1. Teng, K.-H., Raju, S., Zhu, D., Lim, J. L. K., Chen, D. S.-H., Ching, E. W. L., Jaibir, S., Joshua, L. E.-Y., Ng, E. J., Chuan, K. C. T., and Lal, A., "An On-Chip 2-D DFT Accelerator Ultrasonic Wavefront for Convolutional Neural Networks.", *2021 IEEE USNC-URSI Radio Science Meeting (Joint with AP-S Symposium)*., pp. 124-125, doi: 10.23919/usnc-ursi51813.2021.9703556
2. D. S. -H. Chen, M. Sarafianou, E. L. C. Wai, J. Sharma, A. Lal and K. T. C. Chai, "A Study of Bonding Materials for GHz Ultrasonic Wavefront Computing," *2022 IEEE International Ultrasonics Symposium (IUS)*, Venice, Italy, 2022, pp. 1-4, doi: 10.1109/IUS54386.2022.9958758.
3. D. S. H. Chen, E. L. C. Wai, Y. X. Yeo, J. Sharma, A. Lal and K. T. C. Chai, "Investigation of Au-AuSn Bonding Below Eutectic Temperature for Gigahertz Bulk Acoustic Wave Transmission," *2022 IEEE 24th Electronics Packaging Technology Conference (EPTC)*, Singapore, Singapore, 2022, pp. 315-320, doi: 10.1109/EPTC56328.2022.10013215.
4. H. K. Kim, N. H. Kim, "Structural investigations of gold-to-gold wafer bonding interfaces", *2004 Materials Science and Engineering: B*, Vol. 110, Issue 1, pp. 64-67, ISSN 0921-5107, doi: 10.1016/j.mseb.2004.03.004.
5. M. Yamamoto, E. Higurashi, T. Suga, R. Sawada and T. Itoh, "Ar+H2 atmospheric-pressure plasma treatment for Au-Au bonding and influence of air exposure on surface contamination," *2017 5th International Workshop on Low Temperature Bonding for 3D Integration (LTB-3D)*, Tokyo, Japan, 2017, pp. 64-64, doi: 10.23919/LTB-3D.2017.7947460.
6. S. Matsuoka, M. Yamamoto, E. Higurashi, T. Suga and R. Sawada, "Low temperature Au-Au surface-activated bonding using nitrogen atmospheric-pressure plasma treatment for optical microsystems," *2015 International Conference on Electronics Packaging and iMAPS All Asia Conference (ICEP-IAAC)*, Kyoto, Japan, 2015, pp. 850-853, doi: 10.1109/ICEP-IAAC.2015.7111132.